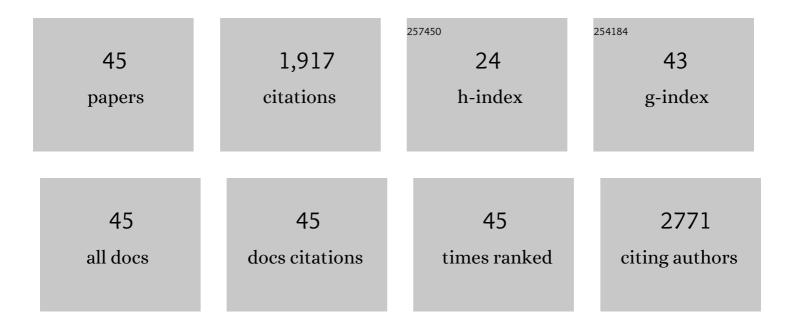
## Steven J Hinder

List of Publications by Year in descending order

Source: https://exaly.com/author-pdf/5987037/publications.pdf Version: 2024-02-01



STEVEN I HINDED

#	Article	lF	CITATIONS
1	Oxygen Rich Titania: A Dopant Free, High Temperature Stable, and Visibleâ€Light Active Anatase Photocatalyst. Advanced Functional Materials, 2011, 21, 3744-3752.	14.9	306
2	Antibacterial properties of F-doped ZnO visible light photocatalyst. Journal of Hazardous Materials, 2017, 324, 39-47.	12.4	187
3	Cu-Doped TiO2: Visible Light Assisted Photocatalytic Antimicrobial Activity. Applied Sciences (Switzerland), 2018, 8, 2067.	2.5	149
4	Highly Efficient F, Cu doped TiO2 anti-bacterial visible light active photocatalytic coatings to combat hospital-acquired infections. Scientific Reports, 2016, 6, 24770.	3.3	145
5	Photocatalytic Properties of g-C3N4–TiO2 Heterojunctions under UV and Visible Light Conditions. Materials, 2016, 9, 286.	2.9	72
6	The Relationship between Reaction Temperature and Carbon Deposition on Nickel Catalysts Based on Al2O3, ZrO2 or SiO2 Supports during the Biogas Dry Reforming Reaction. Catalysts, 2019, 9, 676.	3.5	72
7	A Systematic Study of the Effect of Silver on the Chelation of Formic Acid to a Titanium Precursor and the Resulting Effect on the Anatase to Rutile Transformation of TiO <sub>2</sub> . Journal of Physical Chemistry C, 2010, 114, 13026-13034.	3.1	71
8	Design Aspects of Doped CeO <sub>2</sub> for Low-Temperature Catalytic CO Oxidation: Transient Kinetics and DFT Approach. ACS Applied Materials & Interfaces, 2021, 13, 22391-22415.	8.0	70
9	Indium-Doped TiO <sub>2</sub> Photocatalysts with High-Temperature Anatase Stability. Journal of Physical Chemistry C, 2019, 123, 21083-21096.	3.1	69
10	Electrodeposited Nanostructured CoFe2O4 for Overall Water Splitting and Supercapacitor Applications. Catalysts, 2019, 9, 176.	3.5	65
11	Energy storage on demand: ultra-high-rate and high-energy-density inkjet-printed NiO micro-supercapacitors. Journal of Materials Chemistry A, 2019, 7, 21496-21506.	10.3	63
12	Electrospun Fibres of Chitosan/PVP for the Effective Chemotherapeutic Drug Delivery of 5-Fluorouracil. Chemosensors, 2021, 9, 70.	3.6	40
13	Nickel Supported on AlCeO3 as a Highly Selective and Stable Catalyst for Hydrogen Production via the Glycerol Steam Reforming Reaction. Catalysts, 2019, 9, 411.	3.5	39
14	A ToF-SIMS investigation of a buried polymer/polymer interface exposed by ultra-low-angle microtomy. Surface and Interface Analysis, 2004, 36, 1575-1581.	1.8	37
15	Ternary Metal Chalcogenide Heterostructure (AgInS <sub>2</sub> –TiO <sub>2</sub> ) Nanocomposites for Visible Light Photocatalytic Applications. ACS Omega, 2020, 5, 406-421.	3.5	36
16	Extremely pseudocapacitive interface engineered CoO@3D-NRGO hybrid anodes for high energy/ power density and ultralong life lithium-ion batteries. Carbon, 2021, 171, 869-881.	10.3	36
17	Optimizing the oxide support composition in Pr-doped CeO2 towards highly active and selective Ni-based CO2 methanation catalysts. Journal of Energy Chemistry, 2022, 71, 547-561.	12.9	36
18	Ce–Sm– <i>x</i> Cu cost-efficient catalysts for H <sub>2</sub> production through the glycerol steam reforming reaction. Sustainable Energy and Fuels, 2019, 3, 673-691.	4.9	34

Steven J Hinder

#	Article	IF	CITATIONS
19	Establishing template-induced polymorphic domains for API crystallisation: the case of carbamazepine. CrystEngComm, 2015, 17, 6384-6392.	2.6	33
20	SIMS fingerprint analysis on organic substrates. Surface and Interface Analysis, 2010, 42, 826-829.	1.8	31
21	Interface analysis and compositional depth profiling by XPS of polymer coatings prepared using ultra-low-angle microtomy. Surface and Interface Analysis, 2004, 36, 1032-1036.	1.8	28
22	Pd Loaded TiO2 Nanotubes for the Effective Catalytic Reduction of p-Nitrophenol. Catalysis Letters, 2016, 146, 474-482.	2.6	28
23	Effect of Pt nanoparticle decoration on the H2 storage performance of plasma-derived nanoporous graphene. Carbon, 2021, 171, 294-305.	10.3	27
24	ToF-SIMS depth profiling of a complex polymeric coating employing a C60 sputter source. Surface and Interface Analysis, 2007, 39, 467-475.	1.8	25
25	Ni Catalysts Based on Attapulgite for Hydrogen Production through the Glycerol Steam Reforming Reaction. Catalysts, 2019, 9, 650.	3.5	23
26	Nanostructured Fe-Ni Sulfide: A Multifunctional Material for Energy Generation and Storage. Catalysts, 2019, 9, 597.	3.5	21
27	Continuous selective deoxygenation of palm oil for renewable diesel production over Ni catalysts supported on Al <sub>2</sub> O <sub>3</sub> and La <sub>2</sub> O <sub>3</sub> –Al <sub>2</sub> O <sub>3</sub> . RSC Advances, 2021, 11, 8569-8584.	3.6	21
28	Design of Waterborne Nanoceria/Polymer Nanocomposite UV-Absorbing Coatings: Pickering versus Blended Particles. ACS Applied Nano Materials, 2018, 1, 3956-3968.	5.0	20
29	High-energy sodium-ion hybrid capacitors through nanograin-boundary-induced pseudocapacitance of Co3O4 nanorods. Journal of Energy Chemistry, 2022, 69, 338-346.	12.9	19
30	Realization of High Energy Density Sodium-Ion Hybrid Capacitors through Interface Engineering of Pseudocapacitive 3D-CoO-NrGO Hybrid Anodes. ACS Applied Materials & Interfaces, 2021, 13, 27999-28009.	8.0	16
31	Magnetic Fe3O4–reduced graphene oxide composite decorated with Ag nanoparticles as electrochemical sensor and self-cleaning material for organic pollutants. Journal of Porous Materials, 2020, 27, 303-318.	2.6	15
32	Ni <sub>2</sub> P Nanoparticles Embedded in Mesoporous SiO <sub>2</sub> for Catalytic Hydrogenation of SO <sub>2</sub> to Elemental S. ACS Applied Nano Materials, 2021, 4, 5665-5676.	5.0	14
33	Exploring Different Binders for a LiFePO4 Battery, Battery Testing, Modeling and Simulations. Energies, 2022, 15, 2332.	3.1	13
34	Surface and interface analysis of complex polymeric paint formulations. Surface and Interface Analysis, 2006, 38, 557-560.	1.8	10
35	Interfacial studies of Al <sub>2</sub> O <sub>3</sub> deposited on 4Hâ€SiC(0001). Surface and Interface Analysis, 2008, 40, 822-825.	1.8	9
36	An investigation of the distribution of minor components in complex polymeric paint formulations using ToF-SIMS depth profiling. Surface and Interface Analysis, 2008, 40, 436-440.	1.8	6

Steven J Hinder

#	Article	IF	CITATIONS
37	New Insights into Crystal Defects, Oxygen Vacancies, and Phase Transition of Ir-TiO2. Journal of Physical Chemistry C, 2021, 125, 23548-23560.	3.1	6
38	Unusual pseudocapacitive lithium-ion storage on defective Co <sub>3</sub> O <sub>4</sub> nanosheets. Nanotechnology, 2022, 33, 225403.	2.6	6
39	Nickel azamacrocyclic complex activated persulphate based oxidative degradation of methyl orange: recovery and reuse of complex using adsorbents. RSC Advances, 2015, 5, 31716-31724.	3.6	5
40	Investigation of Chemical and Physical Surface Changes of Thermally Conditioned Glass Fibres. Fibers, 2019, 7, 7.	4.0	4
41	Polymer brush lubrication of the silicon nitride–steel contact: a colloidal force microscopy study. RSC Advances, 2017, 7, 42667-42676.	3.6	3
42	Structural Investigation of the Carbon Deposits on Ni/Al2O3 Catalyst Modified by CaO-MgO for the Biogas Dry Reforming Reaction. , 2020, 2, .		3
43	Unravelling the Impact of Ta Doping on the Electronic and Structural Properties of Titania: A Combined Theoretical and Experimental Approach. Journal of Physical Chemistry C, 2022, 126, 2285-2297.	3.1	2
44	A growth mechanism for carbon nanotubes using metal oxides as catalysts. Surface and Interface Analysis, 2018, 50, 734-743.	1.8	1
45	Metal-Free Phosphated Mesoporous SiO2 as Catalyst for the Low-Temperature Conversion of SO2 to H2S in Hydrogen. Nanomaterials, 2021, 11, 2440.	4.1	1